University of Massachusetts Boston
**ScholarWorks at UMass Boston**

Physics Faculty Publications

Physics

5-28-2001

# Phonon-pumped terahertz gain in n-type GaAs/AlGaAs superlattices

Greg Sun
*University of Massachusetts Boston*, greg.sun@umb.edu

Richard A. Soref
*Air Force Research Laboratory, Hanscom Air Force Base*

Follow this and additional works at: http://scholarworks.umb.edu/physics_faculty_pubs

Part of the Physics Commons

# Phonon-pumped terahertz gain in n-type GaAs/AlGaAs superlattices

Gregory Sun and Richard A. Soref

## Related Articles

## Additional information on Appl. Phys. Lett.

# Phonon-pumped terahertz gain in *n*-type GaAs/AlGaAs superlattices

Gregory Sun[a)]
*Department of Physics, University of Massachusetts at Boston, Boston, Massachusetts 02125*

Richard A. Soref
*Sensors Directorate, Air Force Research Laboratory, Hanscom Air Force Base, Massachusetts 01731*

Local population inversion and far-IR gain are proposed and theoretically analyzed for an unbiased *n*-doped GaAs/Al$_{0.15}$Ga$_{0.85}$As superlattice pumped solely by phonons. The lasing transition occurs at the Brillouin zone boundary of the superlattice wave vector $k_z$ between the two conduction minibands CB1 and CB2 of the opposite curvature in $k_z$ space. The proposed waveguided structure is contacted above and below by heat sinks at 300 K and 77 K, respectively. Atop the superlattice, a heat buffer layer confines longitudinal optical phonons for enhanced optical-phonon pumping of CB1 electrons. A gain of 345 cm$^{-1}$ at 4.5 THz is predicted for a doping density of 2.8 $\times 10^{16}$ cm$^{-3}$. © *2001 American Institute of Physics.* [DOI: 10.1063/1.1376432]

The phonon-pumped laser (PPL) is a radical kind of semiconductor interminiband laser that uses a temperature gradient and optical phonons to excite carriers from the ground-state miniband of a superlattice to an excited miniband. The PPL does not utilize optical pumping or electrical pumping: it has no electrical contacts and operates under the flat-band condition. In a recent manuscript,[1] we proposed a PPL design for the valence minibands of a SiGe/Si superlattice. In this letter, we propose and analyze phonon pumping of a *n*-doped GaAs/AlGaAs superlattice. We show, via calculations, that significant gain appears feasible at THz frequencies—gain that is potentially sufficient for lasing.

Figures 1 and 2 show, respectively, the cross sectional end view and the perspective view of our proposed GaAs THz PPL. The device structure is an edge-emitting metal-coated surface-plasmon strip waveguide that is sandwiched between a warm heat sink at temperature $T_2$ and a cool heat sink at temperature $T_1$. The sinks contact the upper and lower gold claddings of the waveguide. The waveguide supports a single transverse magnetic (TM)$_0$-like mode and has cleaved ends to form a Fabry–Perot resonator. Refering to Fig. 1, the undercoated substrate is (100) GaAs. On it, a buffer layer of undoped GaAs is grown in order to increase the waveguide thickness to several micrometers if the epitaxy machine limits the superlattice (SL) stack height to ~1 $\mu$m. Next, a ~100 period *n*-doped GaAs/Al$_{1-x}$Ga$_x$As superlattice is grown, followed by growth of a second undoped GaAs waveguide spacer layer. Then a heat buffer layer (HBL) is deposited on the structure, followed by deposition of a metal film. Optic and acoustic phonons are launched from the GaAs substrate and travel upward through the SL towards the HBL. The HBL material is chosen so that its optical phonon spectra are different from those of the SL. Consequently, as optical phonons reach the HBL interface, the discontinuity in spectra causes optical phonons to be reflected back down to the SL, thereby confining those phonons in the waveguide; whereas the up-traveling acoustic phonons penetrate through the HBL and are lost. For the

present materials system, we believe that an AlAs layer will act as an adequate HBL.

The inset in Fig. 1 shows the effective temperatures of optical and acoustic phonons, $T_0$ and $T_a$ respectively, as a function of $z$. Using heat-diffusion equations, a detailed analysis[1] shows that $T_0$ is maintained nearly equal to $T_2$ across the device structure up to the HBL as shown in Fig. 1. However, $T_a$ drops steadily from $T_2$ down to $T_1$ across the structure. The SL is located closer to the $T_1$ end, as shown. There, a large difference in effective temperatures $T_0$ and $T_a$ exists. This provides effective pumping of the ground-state electrons of the SL by longitudinal optical (LO) phonons. The next step in obtaining a THz laser is to use quantum engineering to design a SL that has, in effect, four levels in its dispersion diagram as well as a large radiative dipole matrix element $\langle u|z|l \rangle$ between the two minibands CB1 and CB2. For CB2-to-CB1 radiation, the $z$ polarization is allowed and the $xy$ polarization is forbidden.

The SL is a simple, square-well SL operating in the flat band condition. The quantum well and barrier widths ($l_w$ and $l_b$, respectively) and the well and barrier Al compositions ($x_w$ and $x_b$, respectively) are chosen so that the spacing between the first two minibands at zone center $E_2(k_z=0) - E_1(k_z=0) = E_{21}(0)$ is slightly less than the optical phonon energy $\hbar\omega_{LO}$ of GaAs (36.2 meV), to facilitate the CB1-to-
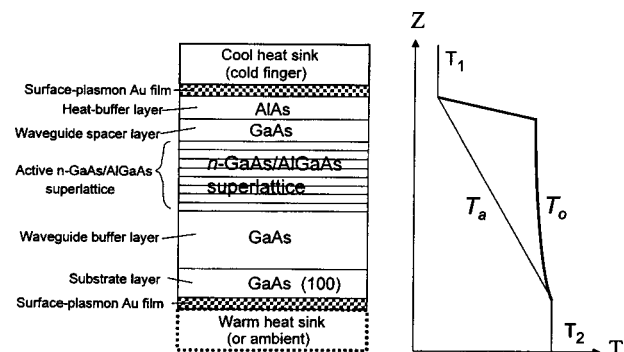


FIG. 1. End view of proposed phonon-pumped laser. Inset shows the effective-temperature distributions of acoustic and optical phonons.

---
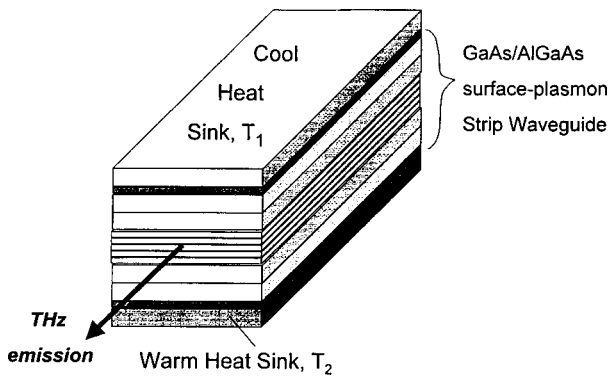
[a)]Electronic mail: gsun@cs.umb.edu

FIG. 2. Perspective view of the Fig. 1 laser.

CB2 optical-phonon pumping process and simultaneously to suppress the optical-phonon assisted CB2-to-CB1 relaxation process given the opposed dispersions for CB2 and CB1 as a function of the SL wave vector $k_z$. We also choose $l_w \gg l_b$ to give large matrix element $\langle u|z|l \rangle$. Using the $\mathbf{k} \cdot \mathbf{p}$ finite-element software from QSA Inc., we found (setting $x_w = 1$) that there is a range of $x_b$, $l_w$, and $l_b$ that produces useful dispersion diagrams. A representative result is given in Fig. 3 for the SL of 210 Å GaAs QWs and 25 Å $Al_{0.15}Ga_{0.85}As$ barriers. The CB electron energy is cited with reference to the top of the HH valence band. The energy minimum of CB1 lies at the SL Brillouin zone center, while the minimum of CB2 occurs at the zone boundary $k_z = \pi/L$, where $L = l_w + l_b$ is the SL period. The choice of a wide GaAs quantum well in the SL produces a large dipole matrix element of 45 Å. Within each miniband, energy relaxation occurs mainly via interaction with acoustic phonons (plus some electron–electron scattering at higher densities). Since $\hbar\omega_{LO} \sim E_{21}(0)$, the population distribution between CB1 and CB2 is determined by the carrier–optical–phonon interaction.[1] We expect that the intraminiband scattering is faster than the interminiband process. As long as that is true, the distribution of carriers within each miniband is characterized by the acoustic phonon temperature $T_a$, while the distribution between minibands is governed by the optical phonon temperature $T_0$. Disregarding the variation in the density of states, we have the total population of electrons $N$ (provided by doping) distributed between the two minibands as



FIG. 3. Energy of the first two conduction minibands vs $k_z$. Quasi-Fermi levels for the $n$-doped ground miniband ($E_{f1}$) and the excited phonon-pumped miniband ($E_{f2}$) are shown.

$$N = N_1(E_{f1}, T_a) + N_2(E_{f2}, T_a), \tag{1}$$

where the population for CB2 ($N_2$) is related to that of CB1 ($N_1$) by

$$N_2 = N_1 \exp(-E_{21}/k_B T_0), \tag{2}$$

where $k_B$ is the Boltzmann constant. The population distribution within each miniband is further characterized by quasi-Fermi levels $E_{f1}$ and $E_{f2}$ shown in Fig. 3, and by $T_a$, assuming quasi-equilibrium is established within CB2 and CB1 due to the fast intra-miniband process

$$N_i(E_{fi}, T_a) = \frac{L}{\pi} \int_0^{\pi/L} dk_z \int_{E_i(k_z)}^{\infty} D(E) f(E, E_{fi}, T_a) dE, \tag{3}$$

where $i = 1, 2$ for CB1 and CB2, respectively, $E_i(k_z)$ is the miniband energy dispersion as a function of SL wave vector $k_z$, and $D(E)$ is the density of states under the approximation of parabolic in-plane dispersion with effective mass $m^*$,

$$D(E) = \frac{m^*}{\pi \hbar^2 L}, \tag{4}$$

and the Fermi–Dirac distribution is

$$f(E, E_{fi}, T_a) = \frac{1}{1 + \exp(E - E_{fi})/k_B T_a}. \tag{5}$$

Due to the upward slope of CB1 and the downward slope of CB2 in Fig. 3, it is possible to achieve local-in-$k_z$ population inversion near the Brillouin zone boundary, even though $N_2$ is always less than $N_1$. Absorption of optical phonons—the pumping process—is shown in Fig. 3 together with the vertical lasing transition at zone edge. The lower laser state at zone edge is rapidly emptied.

The energy of the lasing transition ($\hbar\omega_L$) in Fig. 3 is 18.5 meV corresponding to a 67 $\mu$m wavelength. The optical gain at this wavelength can be calculated as[2]

$$\gamma = \frac{2e^2 |\langle l|z|u \rangle|^2}{n\epsilon_0(\hbar\Gamma)} \frac{2\pi}{\lambda_0} (N_u - N_l), \tag{6}$$

where $e$ is the electronic charge, $(N_u - N_l)$ is the population difference between the upper and lower laser states, $n$ is the refractive index of the SL, $\epsilon_0$ is the permittivity of free space, $\hbar\Gamma$ is the full width at half maximum linewidth of the lasing line, and $\lambda_0$ is the free space wavelength. Our calculations indicate that $\langle u|z|l \rangle$ is 45 Å and we estimate that $\hbar\Gamma$ is 1 meV. Then, with the aid of Eqs. (1)–(6), we predict the 4.5 THz gain as a function of $N$. Our result is shown in Fig. 4 for the temperatures $T_0$ and $T_a$ maintained at 300 K and 77 K, respectively. The gain is positive for a wide range of $N$, and the peak gain of $\gamma = 345$ cm$^{-1}$ is obtained at a doping density of $2.8 \times 10^{16}$ cm$^{-3}$. Keeping $T_0$ at 300 K, preliminary estimates indicate that the gain in Fig. 4 decreases monotonically as $T_a$ is increased from 77 to 150 K.

We wish to point out that, in addition to CB lasers, there are two practical possibilities for valence subband PPLs. The first approach is to ''engineer'' an inverted effective mass for the LH1 miniband as a function of in-plane wave vector $k_x$ or $k_y$. As described earlier,[3,4] this is done via a HH2–LH1 repulsion. Then, the PPL is obtained by making $E(LH1,0) - E(HH1,0) \sim \hbar\omega_{LO}$. This PPL would be a VCSEL since
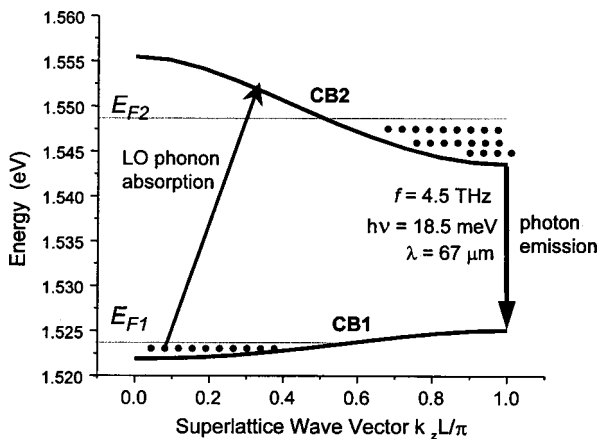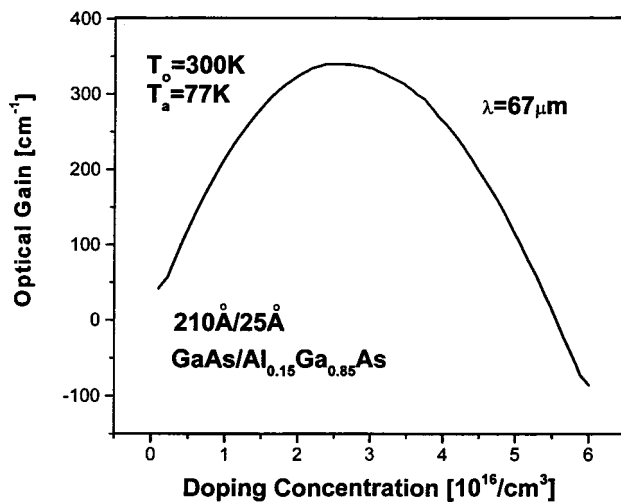
FIG. 4. Calculated optical gain for the Fig. 1 device as a function of doping density.

the allowed LH1–HH1 transition is $xy$ polarized. Here, multilayer dielectric mirrors would replace the plasmon layers and the cool heat sink would be transparent to the surface-normal THz emission. The second possibility is a HH2–HH1 PPL, as discussed for SiGe/Si.[1] Here, HH2 and HH1 curve towards each other versus $k_2$ as desired, although the intervening LH1 curve runs parallel to HH1. In that case, the LH1–HH1 radiative interaction is negligible because the TM-polarized cavity selects HH2-HH1.

The valence-or-conduction miniband PPL principle applies to a variety of IV–IV, III–V, and II–VI semiconduc-

tors that have either zincblende or wurtzite lattices. We have estimated the photon energy, $\hbar\omega_L$, for a few examples of PPL semiconductor SL systems that have $E_{21}(0)$ $\sim 0.95\,\hbar\omega_{LO}$ and $\hbar\omega_L \sim 0.60\,\hbar\omega_{LO}$. We choose a quantum well composition that is close to the barrier composition so that the well depth is roughly $2\hbar\omega_{LO}$. From the semiconductor literature, it is found that the LO optical phonon energy at 300 K is 110.1 meV for AlN (wurtz), 42.2 meV for AlSb (zb), and 43.6 meV for ZnS (zb). Then, we predict the following PPL radiative energies ($\hbar\omega_L$): 66 meV for $Al_{1-x}Ga_xN/AlN$, 25 meV for $Al_{1-x}Ga_xSb/AlSb$, and 26 meV for $ZnS_{1-x}Se_x/ZnS$.

In conclusion, we have theoretically investigated the possibility of local-in-$k_z$ population inversion and THz gain in an unbiased flat-band GaAs/AlGaAs SL pumped by phonons only. A lateral temperature gradient is created across the SL using warm and cool heat sinks that contact the structure. An AlAs heat buffer layer reflects optical phonons back into the SL, making $T_0 > T_a$ for interminiband pumping by phonons. At $T_0 = 300$ K and $T_a = 77$ K, a gain of $345\,\mathrm{cm}^{-1}$ at 4.5 THz is predicted for 210 Å/25 Å $GaAs/Al_{0.15}Ga_{0.85}As$ at $2.8 \times 10^{16}\,\mathrm{cm}^{-3}$ $n$-type doping. The PPL principle applies to a variety of IV–IV, III–V, and II–VI semiconductors.

[1] G. Sun, R. A. Soref, and J. B. Khurgin, IEEE J. Sel. Top. Quantum Electron. (to be published).
[2] G. Sun and J. B. Khurgin, IEEE J. Quantum Electron. **29**, 1104 (1993).
[3] L. Friedman, G. Sun, and R. A. Soref, Appl. Phys. Lett. **78**, 401 (2001).
[4] R. A. Soref, L. Friedman, G. Sun, M. J. Noble, and L. R. Ram-Mohan, Proc. SPIE **3795**, 516 (1999).